Mechanical Properties of Polypropylene/Clay Nanocomposites: Effect of Clay Content, Polymer/Clay Compatibility, and Processing Conditions

J. A. Tarapow,[1] C. R. Bernal,[2] V. A. Alvarez[1]

[1]Research Institute of Material Science and Technology (INTEMA), Engineering Faculty, National University of Mar del Plata, B7608FDQ Mar del Plata, Argentina
[2]Advanced Materials Group, INTECIN (UBA-CONICET), Department of Mechanical Engineering, Engineering Faculty, University of Buenos Aires, C1063ACV Buenos Aires, Argentina

ABSTRACT: In this work, polypropylene/clay nanocomposites with 0.5, 1, 3, and 5 wt % of montmorillonite (MMT) (unmodified clay) were prepared by intensive mixing at 50 rpm and 10 min of mixing. For the highest clay content (5 wt %), the initial materials or the processing conditions were changed to study their independent effect. On one hand, 10 wt % of PP-*graft*-MA (PP-*g*-MA) was incorporated or MMT was replaced by organomodified clays (C10A and C30B). On the other side, for the initial system, the speed of rotation (100 and 150 rpm) and the mixing time (5 and 15 min) were altered. In all cases, the state of the clay inside the matrix (DRX), the degree of dispersion in the micro (SEM) and nano (TEM) scales, and the rheological and mechanical properties were analyzed. It was found that the stiffness increased with clay content, whereas tensile and impact strength did not significantly change. Although intercalated structures were observed in the composites with unmodified clay, in the composites with modified clay or PP-*g*-MA, improved dispersion of clay in PP was found. The mechanical properties increased accordingly. The degree of dispersion of the filler in the matrix appeared to be unaffected by the changes in the processing conditions introduced. Finally, the elastic modulus was modeled by using an effective filler-parameter model based on Halpin–Tsai equations, which also allowed estimating the relative degree of dispersion. © 2008 Wiley Periodicals, Inc. J Appl Polym Sci 111: 768–778, 2009

Key words: nanocomposites; processing conditions; polypropylene; morphology; mechanical properties

INTRODUCTION

Polypropylene (PP) is a useful commodity plastic with good mechanical and barrier properties to water. It is one of the most widely used polymeric materials in large volume. However, its applications are limited because of its poor barrier properties to oxygen, as well as it has the disadvantage of being quite brittle at room temperature and exhibiting poor resistance to crack propagation.[1] To compete with engineering plastics, the incorporation of fillers or reinforcements to PP is often required. In particular, reinforcing this polymer with nanoclays in the adequate conditions can lead to nanomaterials with improved mechanical, thermal, and barrier properties as well as with higher dimensional stability.[2]

After clay or montmorillonite (MMT) is incorporated to a polymer, it can achieve different states. If clay layers remain unseparated, they are called tac-toids. If a small amount of polymer moves into the gallery spacing between clay platelets causing less than 20–30 Å separation between them, the clay is said to be intercalated. If the polymer separates the clay platelets by 80–100 Å or more, exfoliation or delamination is obtained. To achieve the best composite performance, a material with delaminated platelets homogeneously distributed in the polymer is often required.[3]

It is well established in the literature[3] that the degree of delamination and the dispersion of MMT platelets in the matrix are not only greatly affected by the chemistry of the clay surface but also by the processing conditions.

PP has essentially nonpolar groups and, so that, intercalation or exfoliation of silicates inside it is very difficult. One possibility to improve the compatibility is to functionalize the polymer by the addition of functional oligomers as compatibilizers. In such field, Usuki et al.[4] have found a technique to prepare PP nanocomposites using a functional oligomer (PP-OH) with polar telechelic OH groups as compatibilizer. In other studies,[5–7] maleic anhydride (MA)-grafted PP has been used. In both cases,

TABLE I
Physical and Mechanical Properties of the Polypropylene Matrix Giving by the Producer

Melt flow index (230°C/2.16 kg)	3.4 g/10 min
Young's modulus	1.45 GPa
Melting point	166°C
Density	0.88–0.92 g/cm^3

the interaction between clay and PP has been improved because of strong hydrogen bonding. Another route to increase the compatibility between PP and the filler is to modify the clay.

Many works on polymer-based nanocomposites have been focused on the importance of chemical modification of clay to improve the compatibility between clay and polymer,[5–7] whereas the importance of processing conditions have been only analyzed in very few articles.[3]

In the case of PP, there are a number of works in the literature about the preparation of nanocomposites via melt blending,[8] which may be the most appealing method for producing nanocomposites for commercial use.[3] Tidjani et al.[9] have studied the effect of oxygen on the preparation of PP-*graft*-MA (PP-*g*-MA) nanocomposites. On the other side, Wang et al.[10] have determined the influence of the shear stress on the clay dispersion in the case of clay processed by dynamic packing injection molding.

The influence of the processing conditions on the properties of nanocomposites has been reported in some works. Dennis et al.[3] have analyzed polyamide 6 (PA6) nanocomposites showing that the properties depend on the combination of the suitable chemical modification of the clays and optimized processing conditions. Incarnato et al.[11] have also studied the influence of the speed of screw rotation in the case of extrusion for PA-based nanocomposites.

The aim of this work was to analyze the effect of clay content, polymer/clay compatibility, and processing conditions on the mechanical properties of PP/clay nanocomposites.

EXPERIMENTAL

Materials

Syndiotactic polypropylene, kindly supplied by Petroquímica Cuyo, Argentina, was used as the matrix. Some of its physical and mechanical properties are shown in Table I. To improve the compatibility between the PP matrix and clay, 10 wt % PP-*g*-MA (Epolene E-43 wax, Eastman Chemical Company, USA) was also added in the formulation of some nanocomposites.

Three different commercially available clays (Cloisite Na$^+$ (MMT), Cloisite 30B® (C30B), and Cloisite 10A® (C10A) purchased from Southern Clay Prod-

ucts, USA) were employed as nanofillers. They were used as received. Their characteristics are shown in Table II.

Nanocomposites preparation

A home-made intensive mixer was used for nanocomposites manufacture. It is a Brabender type intensive mixer. It has an engine of 5 HP, two counter-rotating rollers, a capacity of 300 cm^3, a temperature range from 30 to 300°C, a speed range from 10 to 300 rpm, and three thermocouples to sense the temperature in the middle and in both walls of the mixer. The processing temperature was set at 180°C. The speed of rotation and the mixing time were initially 50 rpm and 10 min, respectively. Four MMT contents: 0.5, 1, 3, and 5 wt % were used. After mixing, 3-mm plaques were compression-molded in a hydraulic press for 10 min at 180°C under a pressure of 5 MPa.

Once the effect of clay content was studied, the initial materials or the processing conditions were changed to explore their independent effect.

Changes in the initial materials

Ten weight percent of PP-*g*-MA was incorporated in the matrix of PP/MMT composites.

C10A or C30B were used as reinforcement instead of unmodified MMT in the nanocomposites.

Changes in the processing conditions

Residence time: Two different mixing times, 5 and 15 min, were used.

Speed of rotation: Two different speeds, 100 and 150 rpm, were used.

TABLE II
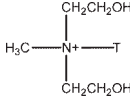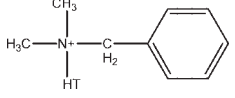Characteristics of the Different Nanoclays Used

Clay	Organic modifier	Modifier concentration (meq/100 g clay)	Specific gravity (g/cm^3)
MMT	None	–	2.86
C30B		90	1.98
C10A		125	1.90

TABLE III
Effect of Clay Content on the Properties of PP/MMT Nanocomposites

Clay content (wt %)	σ_u (MPa)	E (GPa)	ε_b (%)	E_{izod} (kJ/m)	X_{cr} (%)
0	33.6 ± 1.0	1.43 ± 0.07	30.8	1.58 ± 0.18	51.0
0.5	33.5 ± 1.5	1.52 ± 0.06	17.6	1.72 ± 0.21	53.4
1.0	34.1 ± 0.6	1.62 ± 0.05	16.3	1.75 ± 0.32	48.8
3.0	33.9 ± 0.8	1.86 ± 0.06	13.1	1.75 ± 0.20	49.7
5.0	32.8 ± 1.9	1.88 ± 0.07	7.2	1.65 ± 0.11	48.2

Testing and characterization

Uniaxial tensile tests were carried out at room temperature (23°C) in a Universal Testing Machine at 5 mm/min (Instron 4467) by following ASTM D 638M-93 standard recommendations. Dumbbell-shaped specimens were used for these tests. Sample dimensions were measured to an accuracy of 0.01 mm. Stress–strain curves were obtained from these tests, and Young's modulus, tensile strength, and elongation at break values were determined from these curves. At least five specimens were tested, and the average values were reported.

Izod impact tests were also performed at room temperature, in a falling weight Fractovis of Ceast at 1 m/s in according with ASTM D 256-93 standard recommendations. The total energy required to fracture the specimen, E_{tot}, was obtained from the total area under the load-displacement curve also normalized by sample dimensions:

$$E_{Izod} = \frac{1}{b.(W - a)} \int_0^{x_{total}} F.dx \qquad (1)$$

where b and W are the thickness and the width of the sample, respectively, and a is the crack length.

Wide angle X-ray scattering (WAXS) was conducted at room temperature on a PW 1710 based diffractometer equipped with CuKα generator (λ = 0.154 nm). Samples were scanned in 2θ ranges from 5° to 60° by a step of 0.035°. The interlayer distance was calculated from the (001) peak by using the Bragg's equation: $n\lambda = 2d.\sin(\theta)$.

The dispersion of clay on the microscopic scale was examined by using a Philips Model JEOL JSM-6460LV scanning electron microscope. Specimens were fractured at cryogenic temperature in liquid air. Then, they were sputter coated with a thin layer of gold before they were observed.

A transmission electron microscope (TEM) JEOL CX II using an acceleration voltage of 80 kV was used to observe the dispersion of clay platelets inside the polymer chains.

Differential scanning calorimetry (DSC) tests were performed in a Shimadzu DSC-50 from 25 to 200°C at a heating rate of 10°C/min under nitrogen (ASTM D3417-83). The degree of crystallinity was calculated from the following equation[12]:

$$X_{cr} (\%) = \frac{\Delta H_f}{w_{PP} \cdot \Delta H_{100}} \cdot 100 \qquad (2)$$

where ΔH_f is the experimental heat of fusion, w_{PP} is the PP weight fraction, and ΔH_{100} is the heat of fusion of 100% crystalline PP, which has a value of 207.1 J/g.[13]

RESULTS AND DISCUSSION

Effect of clay content

As it was described in the Experimental section, the nanocomposites used in the study for analyzing the effect of clay content were obtained by mixing PP and MMT for 10 min at 50 rpm. Table III shows the tensile properties for PP and the nanocomposites as a function of clay content. Neat matrix exhibited a high value of Young's modulus (1.43 ± 0.07 GPa), which can be related to the relatively high degree of crystallinity (around 50%) observed (Table III). It is also seen in Table III that while tensile strength and Izod impact strength remained almost constant with clay content, the modulus increased and the elongation at break decreased as a function of clay wt %. The latter was the expected result from the incorporation of more rigid inorganic filler (clay) to PP.[14]

The lack of improvement of tensile strength and impact toughness could be attributed to poor interfacial adhesion between the PP matrix and unmodified clay.

In addition, the general trend indicated that further increase in clay content above 5 wt % would not conduct to a significant change in the stiffness probably as a result of the higher agglomeration of clay for these higher clay contents as it will be shown later.

It is also important to note that there exist several factors that can influence the mechanical properties. The degree of crystallinity would be one of these factors. It could affect mechanical properties because a higher fraction of crystals leads to an increase in

the strength and stiffness of the material.[15] However, as it can be observed in Table III, the degree of crystallinity of PP remained almost constant (50.2 ± 2.1) when clay was incorporated and also as a function of clay content. Hence, the effect of crystallinity on the mechanical properties could be passed up for the nanocomposites studied in this work.

A critical parameter to achieve the best performance of our polymer/clay nanocomposites, provided the incorporation of clay does not induce any defects, seems to be the dispersion of clay in the PP matrix as it will be demonstrated later.

To identify intercalated structures, X-ray diffraction analysis was used. In polymer/clay nanocomposites, the interlayer spacing can be determined because of the repetitive multilayer structure. When polymer chains are intercalated, the interlayer spacing generally increases, shifting the diffraction peak to lower angle. When the dispersion of clay becomes higher, no more diffraction peaks are visible in the X-ray diffractograms because of a large spacing between the layers or because nanocomposites do not present ordering anymore, i.e. exfoliation. Besides these two structures, other intermediate organizations can be present (showing both intercalation and exfoliation). In this case, a broadening of the diffraction peak is often observed.[8]

Figure 1 shows the DRX patterns of the matrix, clay, and two nanocomposites (with the lowest and the highest clay content investigated). It is observed in this figure that the position of d_{001} peak was shifted to lower angles probably because of the intercalation of the polymer chains between the clay platelets (inside the galleries) but no evidence of exfoliation could be found.

Figure 2 presents SEM micrographs for the matrix and the nanocomposites with different clay content. In the case of the matrix [Fig. 2(a)], the fracture surface is typical of a brittle material, and this behavior was not significantly changed by the presence of clay. For low clay contents up to 1 wt % [Fig. 2(b,c)], no clay aggregates were observed suggesting a good dispersion of clay in the PP matrix. For higher clay contents [Fig. 2(d,e)], on the other hand, some aggregates were found. However, the distribution of these structures seemed to be quite-uniform. The presence of clay aggregates could be responsible for the lower comparative increment in the Young's modulus as the clay content increased above 1 wt %, and the expected trend that further increase in clay content above 5 wt % would not conduct to a significant change in the stiffness, as stated earlier.

Figure 3 presents TEM micrographs of nanocomposites with 0.5, 1, 3, and 5 wt % of clay. Considering that the dark are the silicate platelets, the presence of unseparated MMT layers (i.e., tactoids) is evident, and some areas where a small amount of
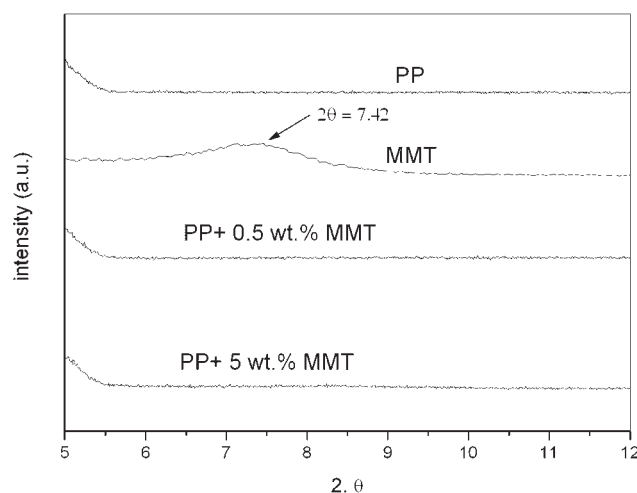

Figure 1 DRX patterns of the matrix, clay, and two nanocomposites with 0.5 and 5 wt % of MMT.

polymer moved into the gallery spacing between the clay platelets are observed. They cause less than 2–3 nm separation between the platelets and are known as intercalated zones. It has been already reported by Dennis et al.[3] that when no compatibility exists between clay and PP, tactoids or intercalants can be obtained but only a partial exfoliation can occur.

Figure 4 shows the rheological properties (measured at 1 Hz) of PP and the nanocomposites with different clay contents. When clay was incorporated (0.5 wt %) both, the storage modulus and the melt viscosity increased respect to the neat matrix in agreement with expectations. It is also observed in Figure 4 that once both parameters (modulus and melt viscosity) reached a maximum value (around 1 wt % of clay), they decreased with clay content. It is well known that the rheological properties of nanocomposites are sensitive to the surface characteristics and the state of dispersion of the second phase.[16] Therefore, the above behavior could be attributed to the presence of agglomerates as well as to the decrease of the polymer molecular weight caused by the increased frictional shear forces of the clays inside the polymer in the intensive mixer, for higher clay contents.

Effect of the compatibility between clay and PP

The mechanical properties (tensile strength, Young's modulus, and impact strength) of nanocomposites with 5 wt % of different clays (MMT, C10A, and C30B) are shown in Figure 5(a–c). The effect of the incorporation of 10 wt % of PP-*g*-MA to the matrix was also included in these figures.

As it was mentioned earlier, for our nanocomposites, the degree of crystallinity remained almost constant (around 50%); hence, this parameter was
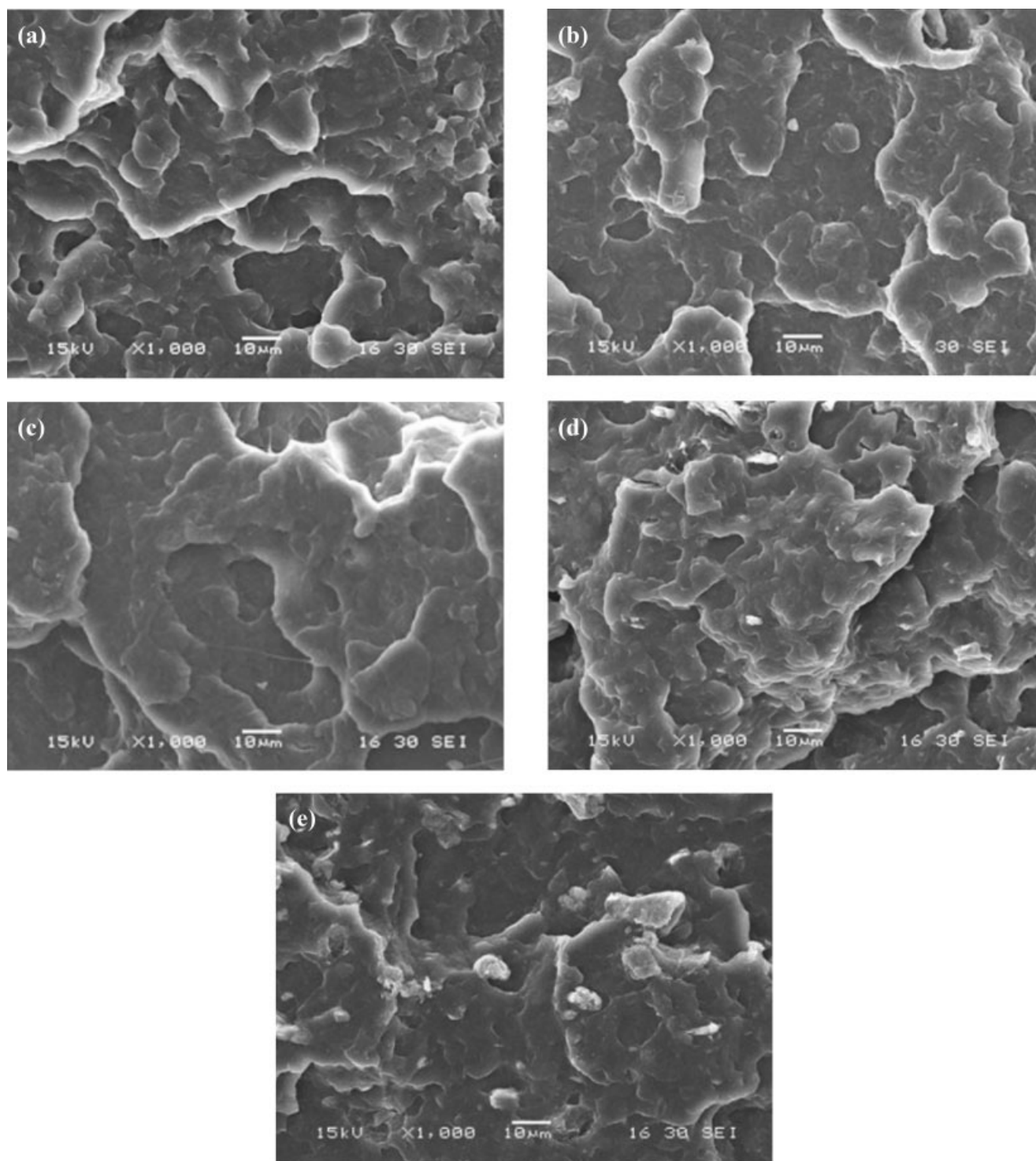
Figure 2 SEM micrographs for: (a) PP; (b) PP + 0.5 wt % of clay; (c) PP + 1 wt % of clay; (d) PP + 3 wt % of clay; and (e) PP + 5 wt % of clay. (Magnification: ×1000).

not expected to have any influence on the results presented here.

It can be observed in Figure 5(a,b) that the incorporation of organomodified clay (C10A and C30B) into PP led to nanocomposites with slightly better tensile strength and stiffness in comparison to the nanocomposites with unmodified clay. On the other side, modification of PP with 10 wt % PP-g-MA did not lead to a significant improvement in tensile properties with respect to the nanocomposite with
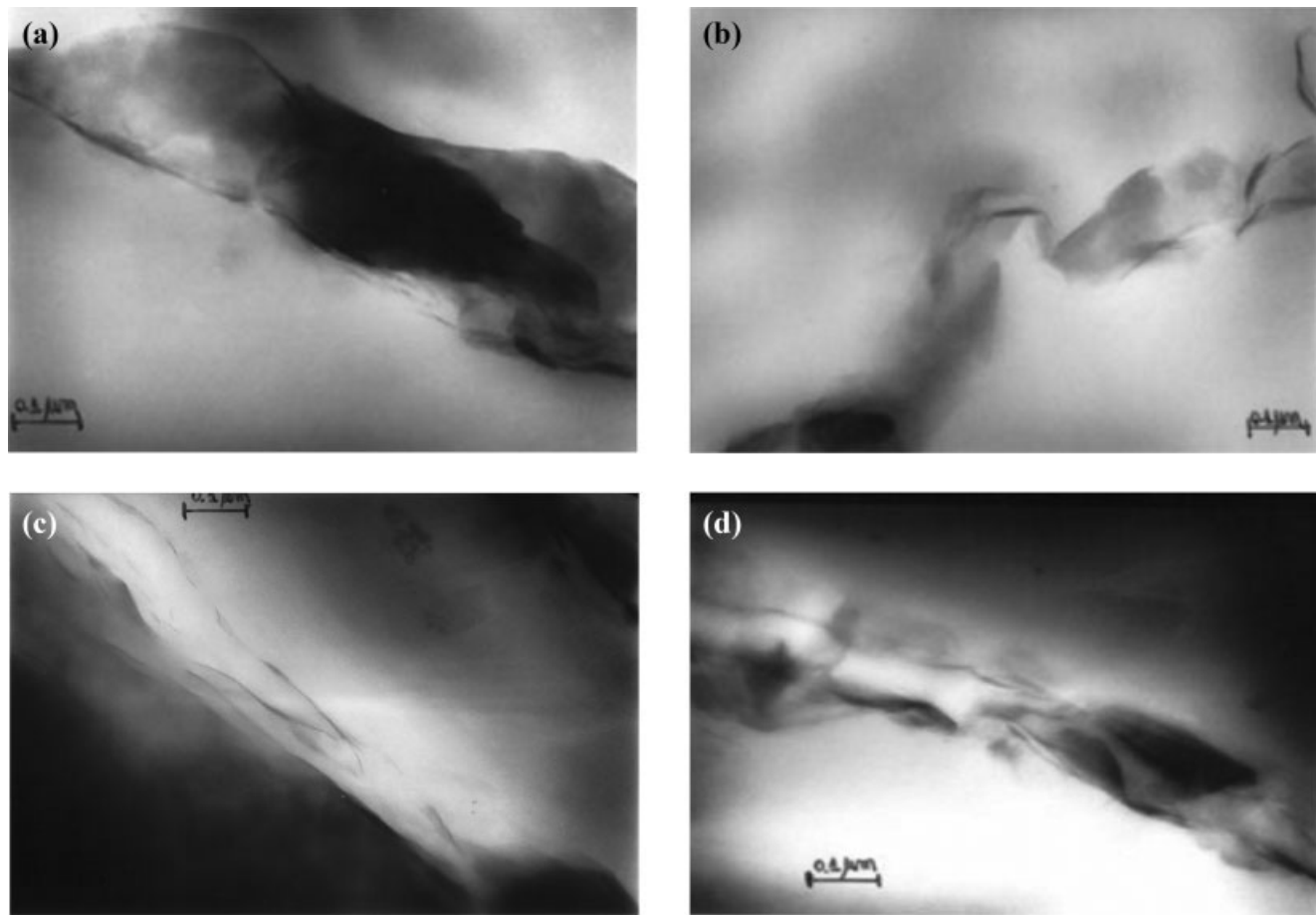
Figure 3 TEM micrographs for: (a) PP + 0.5 wt % of clay; (b) PP + 1 wt % of clay; (c) PP + 3 wt % of clay; and (d) PP + 5 wt % of clay.

neat PP. It is important to note that when PP-*g*-MA nanocomposites were consider, the matrix was PP-*g*-MA whose properties might be differ from those of the neat PP, thus changing the reinforcement effect.

Nevertheless, the differences observed in tensile properties were not relevant taking into account the standard deviations of experimental values. Hence, no important changes in the tensile properties as a function of matrix/clay compatibility were found. A possible reason for this behavior is that, despite of the matrix/clay compatibility, in all cases, it was not possible to achieve complete exfoliation of the clay inside the polymeric matrix, and therefore reinforcement effect was reduced.

However, impact toughness was significantly improved as a result of either clay or matrix modification [Fig. 5(c)], especially for the composites with C10A clay. An enhancement of Izod impact toughness in PP/clay nanocomposites has been attributed in the literature[2,17] to the presence of intercalated or exfoliated clay layers able to hinder the crack path caused by impact. Therefore, the stress can be dispersed by those layers having higher stiffness and strength than the matrix, and hence increasing

impact strength. This effect has been reported to be more significant for higher interaction between PP and clay. This is the case of the nanocomposites with C10A clay.[18]

Figure 6 shows the DRX spectra for unmodified clay (MMT) and the organomodified clays, i.e., C30B
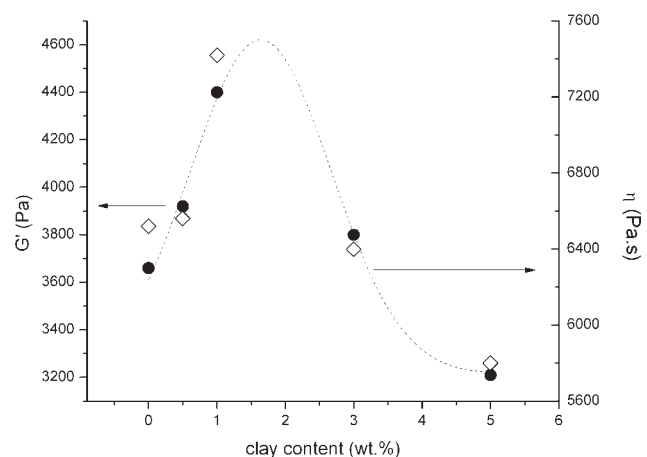

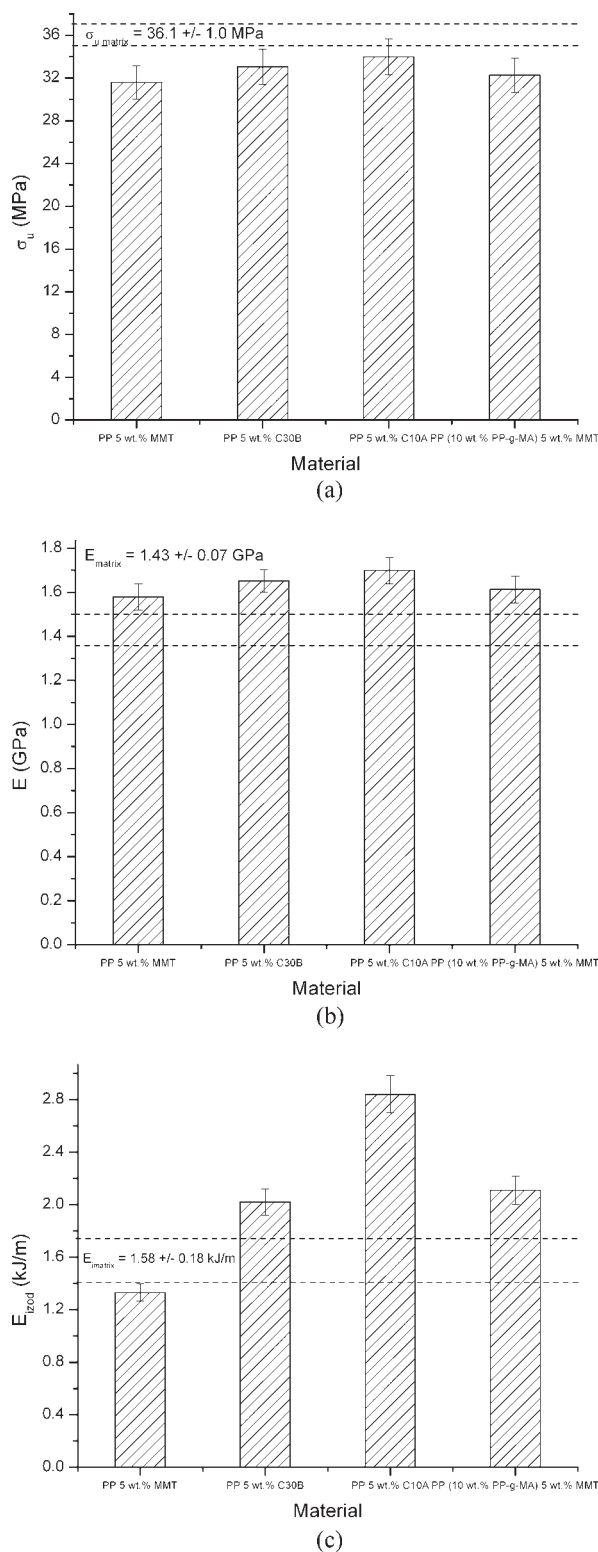**Figure 4** Rheological properties (G' and η) of PP and nanocomposites with different clay contents.

Figure 5   (a) Tensile strength; (b) Young's modulus; and (c) impact energy of nanocomposites with 5 wt % of MMT, C10A, and C30B and influence of PP-*g*-MA incorporation.

and C10A (the *d*-spacing was also included in the figure). It can be observed that in modified clays, the d_{001} peak shifted to lower angles, corresponding to an increase on the basal spacing of the clays by

exchange of interlayer sodium with ammonium cations. Again, the peak was not clear for the nanocomposites (not shown), suggesting the intercalation/exfoliation of the polymer chains inside the galleries.

DRX patterns for PP-*g*-MA/PP/MMT nanocomposites (not shown) exhibited the same behavior than that of the PP/MMT nanocomposites. The interlayer spacing could not be determined because of the peak broadening. However, it should be noted that there is a peak characteristic of interlayer spacing, even it is small. The decrease in intensity and the broadening of peaks could indicate that the stacks of layered silicates became more disordered, while maintaining a periodic distance. In addition, the decrease in intensity could be the result of a partial exfoliation of layered silicates.

Figure 7 shows TEM micrographs for the different nanocomposites with modified matrix or filler. As it can be observed in this figure, the dispersion of clay nanoparticles in the PP matrix was clearly improved by using modified clays, especially for the clay C10A, which is the most hydrophobic and led to the highest polymer-clay compatibility.[18] The results of tensile and impact properties were also in agreement with this tendency (Fig. 5). The higher the compatibility and the better the dispersion of clay in PP, the better will be the mechanical properties.

PP-*g*-MA/PP/MMT and especially PP/C10A nanocomposites show a higher degree of disordered structures and exfoliated layers than PP/MMT nanocomposites. It can also be observed how the structure of these nanocomposites is intermediate between an intercalated and an exfoliated state, with stacks of disordered layers of around 200 nm and smaller aggregates containing between 2 and 10 clay platelets. The compatibility between clay and the matrix increased leading to a higher degree of exfoliation.[3]
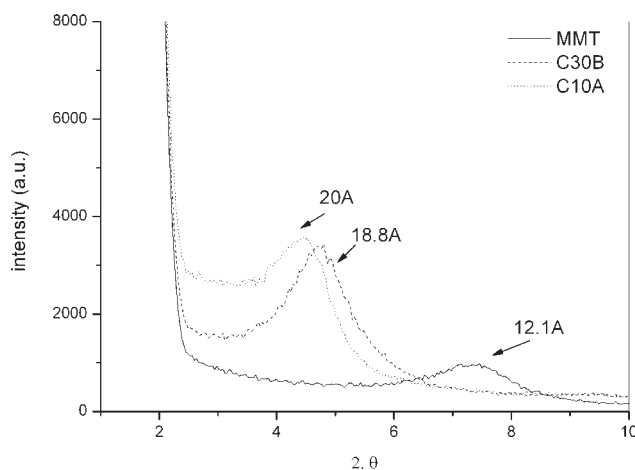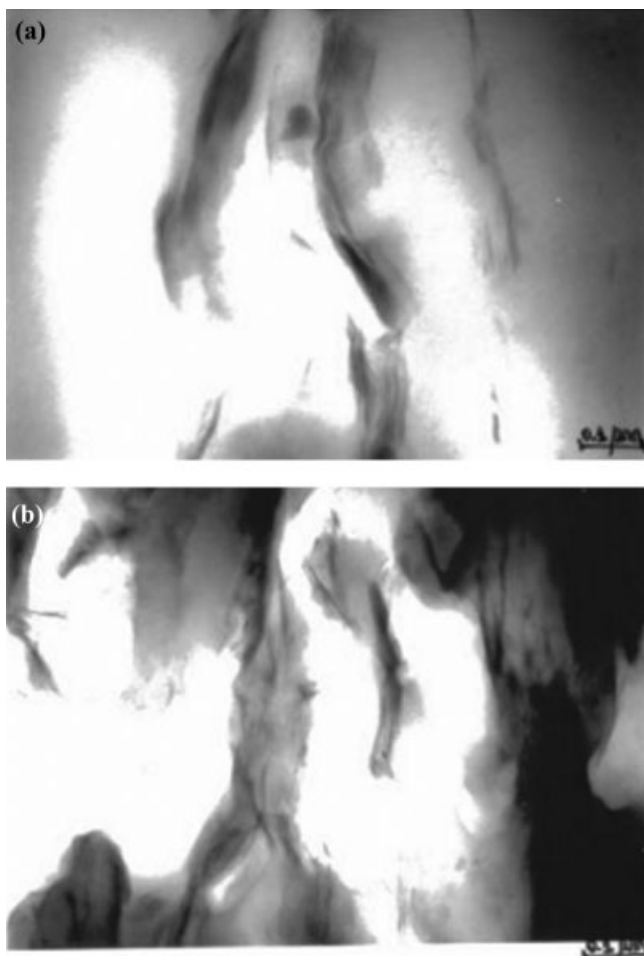

Figure 6   DRX spectra for MMT, C30B, and C10A.

Figure 7 TEM micrographs for: (a) PP + 5 wt % C10A and (b) PP (10 wt % PP-*g*-MA) + 5 wt % MMT.

Because of the low grafting percentage of PP-*g*-MA, which is usually about 0.5–2%, a low content of PP-*g*-MA is not expected to significantly improve the compatibility between clay and PP. On the other hand, the excess of PP-*g*-MA may lead to deterioration of the properties of the nanocomposite because of the low molecular weight of the PP-*g*-MA. To obtain effective intercalation, a high graft polymer/organoclay ratio (3 : 1) is often needed[5,19–21] but this ratio significantly increases the cost of the finished product. Furthermore, as the properties of the matrix are substantially different from those of neat PP, the analysis of the effects of the organoclay on the material properties is very complex.

Effect of processing conditions

The effect of processing conditions on the morphology and the mechanical properties of PP/MMT nanocomposites was studied by changing the residence time or the speed of rotation in the mixer, independently.

Figure 8 shows the effect of mixing time on the mechanical properties of PP 5 wt % MMT nanocomposites. As it can be seen in this figure, no significant differences among the nanocomposites obtained at different mixing times were observed. In general, the dispersion of the clay inside the PP matrix and the degree of delamination could be improved by increasing the residence time in the mixer. The latter being a consequence of the diffusion of the polymer chains into the clay galleries. However, delamination would not have occurred in our nanocomposites as a result of the incompatibility between unmodified clay and PP, but only changes in the size of tactoits or intercalants were expected.[3]

From the analysis of SEM micrographs (Figs. 3, 9), it was determined that clay aggregates of similar sizes were present irrespective of the mixing time used. This result is in agreement with the results of mechanical properties.

Another processing parameter analyzed in this study was the speed of rotation in the intensive mixer. Figure 10 shows the effect of the speed of rotation on the mechanical properties of PP/5 wt % MMT. As in the case of the mixing time, the effect of the speed of rotation was negligible.

TEM micrographs of the PP/MMT nanocomposites studied in this work are shown in Figure 11. In this figure, some clay agglomerates can be observed.

From the results presented earlier, it is suggested that changes in the processing conditions did not induce significant changes in the dispersion of clay into PP and also in the state of clay, which was not able to achieve a high degree of intercalation or exfoliation because of the poor compatibility between unmodified clay (MMT) and pure PP. Therefore, no significant changes in the mechanical properties of the nanocomposites were obtained by changing the processing conditions.

As it can be inferred from the morphological characterization, a high degree of intercalation or exfoliation of clay could be achieved only when a high compatibility between polymer and clay existed. The PP nanocomposites containing PP-*g*-MA showed an intercalated or exfoliated structure and a sensible enhancement of mechanical properties. PP nanocomposites without compatibilizer, on the other hand, showed the presence of intercalated zones and some tactoids and lower improvement of mechanical properties as stated earlier.

Our results also showed that the impact strength values of nanocomposites with modified clay or grafted PP were higher than those of pure PP. This is a great advantage of nanofillers with respect to traditional micrometric fillers, which generally cause a sensible decrease of this property. Using PP-*g*-MA/PP/MMT nanocomposites, processed at suitable conditions, a material that combines high stiffness and good ductility could be obtained.
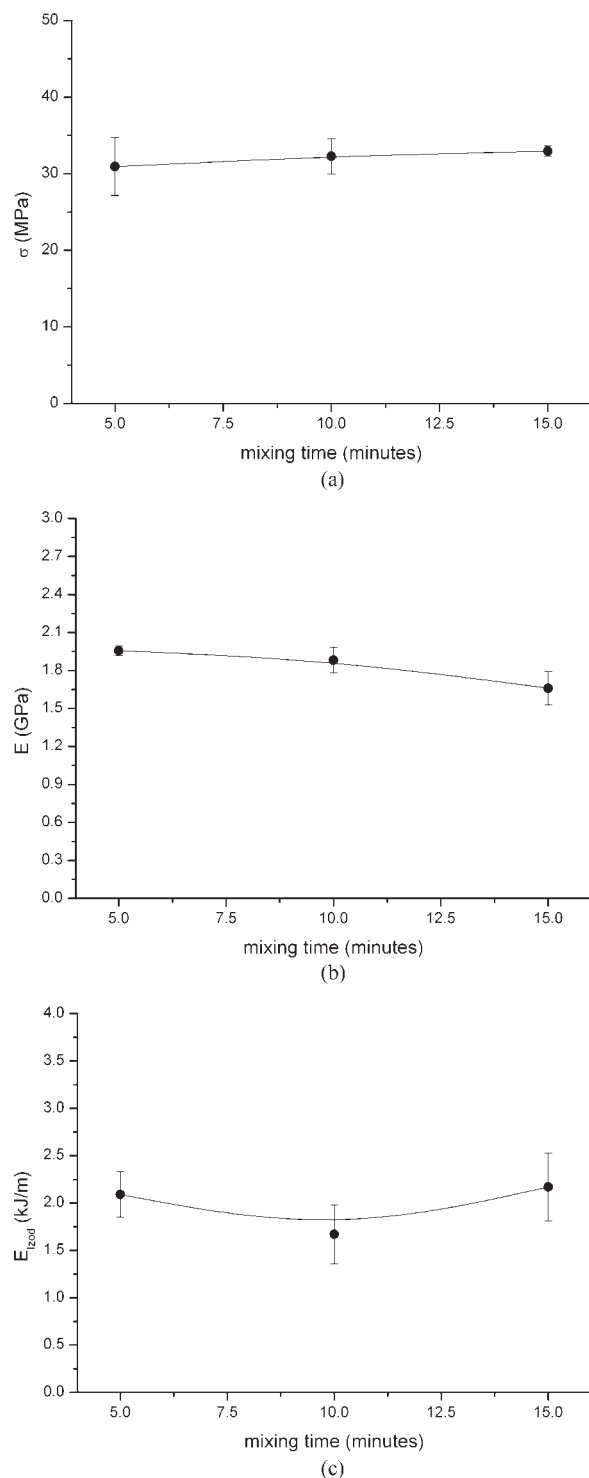
Figure 8 (a) Tensile strength; (b) Young's modulus; and (c) impact energy of nanocomposites with 5 wt % of MMT prepared with different mixing times.

Modeling of mechanical properties

Halpin–Tsai micromechanics-based model

Micromechanical-based models have been used in the case of composites to analyze the effect of filler's structural parameters, such as shape, aspect ratio,

and orientation on the mechanical properties of a neat matrix.[22,23] Although these micromechanical models cannot be used to fully account for the exact mechanical behavior of polymer nanocomposites, they generally give satisfactory correlations.

Tucker and Liang[24] have reported the application of several models for fiber-reinforced composites demonstrating that the Halpin–Tsai theory[25] gives reasonable predictions in the case of the modulus.

By using that model, the longitudinal engineering modulus (E_{11}) can be calculated as:

$$\frac{E_{11}}{E_m} = \frac{1 + 2\left(l/t_p\right)\eta\phi_f}{1 - \eta * \phi_f} \tag{3}$$

where ϕ_f, l, t_p, and E_f are the volume fraction, the length, the thickness, and the modulus of the filler, respectively, E_m is the modulus of the matrix; and

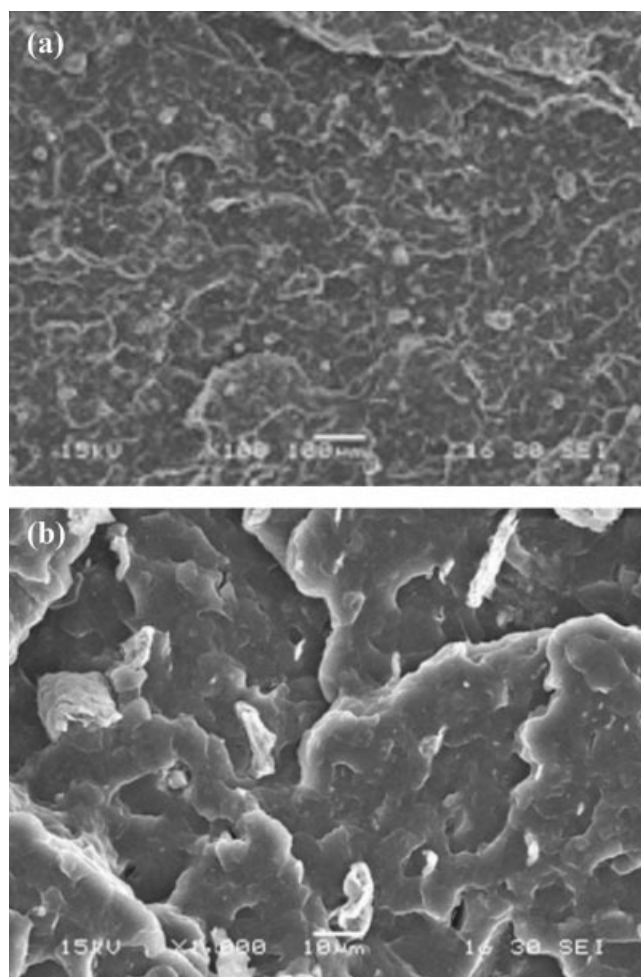$$\eta = \frac{E_f/E_m - 1}{E_f/E_m + 2\left(l/t_p\right)}. \tag{4}$$

Figure 9 SEM micrographs for PP + 5 wt % MMT mixed (a) 5 and (b) 15 min in the intensive mixer. (Magnification: ×1000).
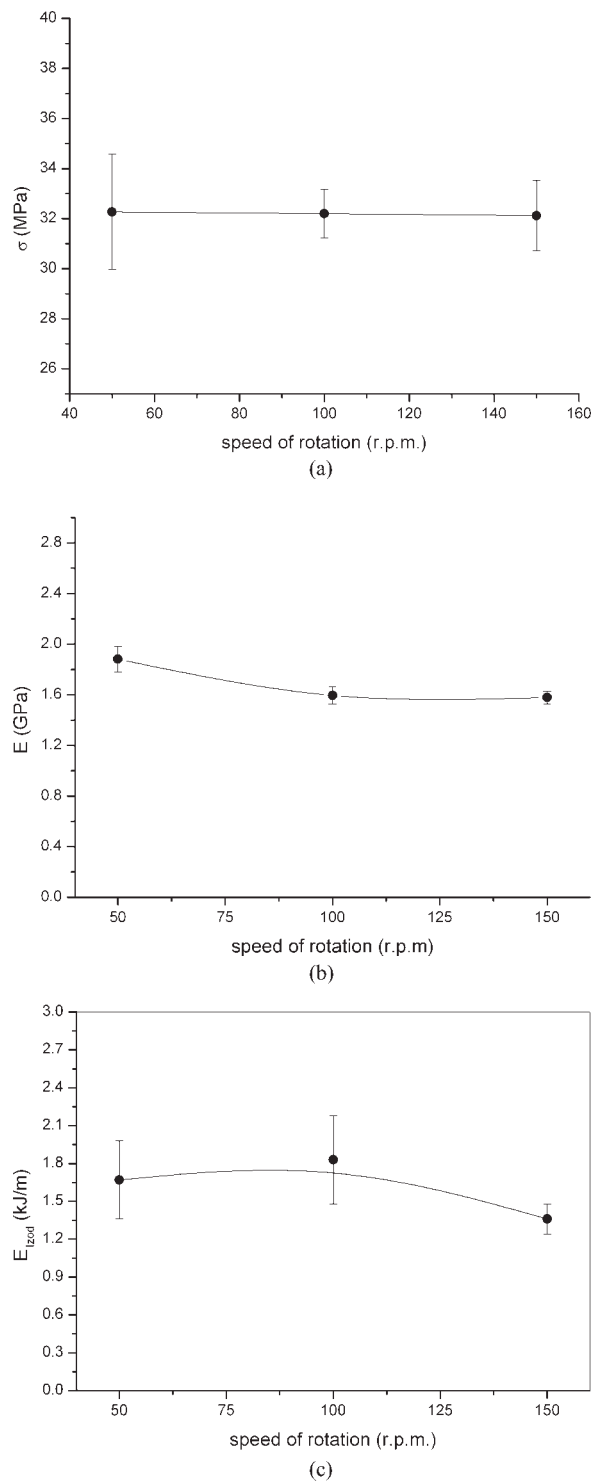
Figure 10 (a) Tensile strength; (b) Young's modulus; and (c) impact energy of nanocomposites with 5 wt % of MMT prepared with different speed of rotation.

can be corrected by considering the morphological parameters of the clay: the number of platelets per stacked clay (n) and the interlayer spacing (d_{001}).

The thickness of the effective filler (t_{eff}) can be expressed as:

$$t_{eff} = (n-1)d_{001} + t_p \qquad (5)$$

The effective filler aspect ratio (α_{eff}), volume fraction (ϕ_{eff}), and modulus (E_f^{eff}) can be written as:

$$\alpha_{eff} = \frac{l}{t_{eff}} = \frac{l}{(n-1)d_{001} + t_p} \qquad (6)$$

$$\phi_{eff} = \frac{\psi_{eff}\lfloor (n-1)d_{001} + t_p \rfloor}{nt_p} \frac{\rho_m}{\rho_f} \qquad (7)$$

$$E_f^{eff} = \frac{nt_pE_f}{[(n-1)d_{001} + t_p]} \qquad (8)$$

where ψ_{eff} is the effective filler weight fraction and ρ_f, ρ_m are filler and matrix densities, respectively.

From the previous model and by using the experimental elastic modulus values, the degree of

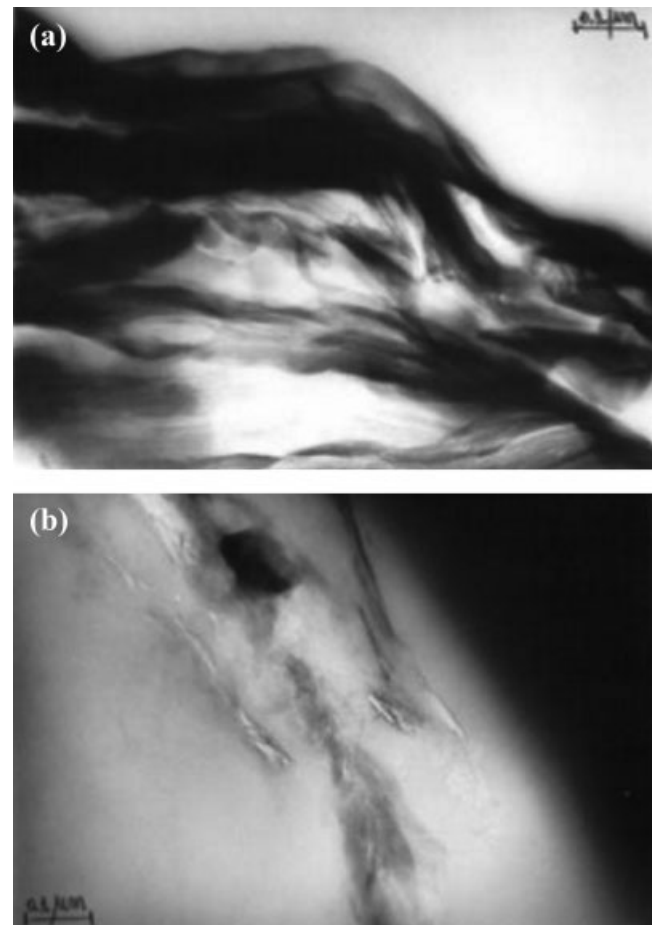**Figure 11** TEM micrographs for PP + 5 wt % MMT mixed 10 min at (a) 100 rpm and (b) 150 rpm in the intensive mixer.

Effective filler-parameters model[26]

The dispersion of clay within a matrix can be described in terms of exfoliation and/or intercalation, which are not taken into account in the classical micromechanical models. The parameters of the filler

TABLE IV
Relative Number of Platelets per Stacked Clay (n_r) from the Effective Filler-Based Micromechanical Model

MMT content (wt %)	n_r
0	N/A
0.5	1.00
1	1.00
3	1.06
5	1.32

dispersion of nanocomposites was estimated. A relative n_r value was calculated as:

$$n_r = \frac{n_i}{n_{\min}} \quad (9)$$

being n_i the real n value and $n_{\min}$ the lowest n value.

Table IV shows n_r values obtained from the use of the model as a function of clay content for PP/MMT nanocomposites. It is clear, from the increase of n_r value, that particles agglomeration became important at 5 wt % of clay. The results of the model are in accordance with the mechanical properties and morphological analysis

CONCLUSIONS

PP/clay nanocomposites were prepared. It was determined that the Young's modulus was improved by the clay incorporation and became higher as a function of clay content. On the other hand, neither the tensile strength nor the impact toughness were enhanced and this could be attributed to poor interfacial adhesion between the PP matrix and unmodified clay. DRX patterns indicated that the polymer chains were intercalated between the clay platelets, whereas no evidence of exfoliation was found. From TEM micrographs, some areas where a small amount of polymer moved into the gallery spacing between the clay platelets were clearly observed. Both results were in accordance with those of mechanical properties. Analyzing the compatibility between clay and matrix (by using different clays or PP-*g*-MA), it was clear than the highest effect (increased mechanical properties and improved dispersion observed by TEM) was obtained for the most hydrophobic clay used (C10A). Nevertheless, the differences in the mechanical properties were not significant when comparing with the standard deviations, except for the impact toughness where a clear increase was observed for the nanocomposite with C10A. The processing conditions showed no important influence on the degree of dispersion or the mechanical properties.

The effective filler-based micromechanical model was useful to estimate the relative degree of dispersion of clay in the PP matrix.

References

1. Montoya, M.; Abad, M. J.; Barral Losada, L.; Bernal, C. J Appl Polym Sci 2005, 98, 1271.
2. Modesti, M.; Lorenzetti, A.; Bon, D.; Besco, S. Polymer 2005, 46, 10237.
3. Dennis, H. R.; Hunter, D. L.; Chang, D.; Kim, S.; White, J. L.; Cho, J. W. Polymer 2001, 42, 9513.
4. Usuki, A.; Kato, M.; Okada, A.; Kurauchi, T. J Appl Polym Sci 1997, 63, 137.
5. Kawasami, M.; Hasegawa, N.; Kato, M.; Usuki, A.; Okada, A. Macromolecules 1997, 30, 6333.
6. Nam, P. H.; Maiti, P.; Okamoto, M.; Kotaka, T.; Hasegawa, N.; Usuki, A. Polymer 2001, 42, 9633.
7. Kato, M.; Usuki, A.; Okada, A. J Appl Polym Sci 1997, 66, 1781.
8. Alexandre, M.; Dubois, P. Mater Sci Eng R 2000, 28, 1.
9. Tidjani, A.; Wald, O.; Pohl, M. M.; Hentschel, M. P.; Schartel, B. Polym Degrad Stab 2003, 82, 133.
10. Wang, K.; Liang, S.; Zhang, Q.; Fu, Q. Polymer 2004, 45, 7953.
11. Incarnato, L.; Scarfato, P.; Russo, G. M.; Di Maio, L.; Iannelli, P.; Acierno, D. Polymer 2003, 44, 4625.
12. Yam, W. Y.; Ismail, J.; Kammer, H. W.; Schmidt, H.; Kummerlöwe, C. Polymer 1999, 40, 5545.
13. Bu, H. S.; Cheng, S. Z. D.; Wunderlich, B. Makromol Chem Rapid Commun 1988, 9, 75.
14. Százdi, L.; Pozsgay, A.; Pukánszky, B. Eur Polym J 2007, 43, 345.
15. Simanke, A. G.; Galland, G. B.; Freitas, L.; da Jornada, J. A. H.; Quijada, R.; Mauler, R. S. Polymer 1999, 40, 5489.
16. Ren, J.; Silva, A. S.; Krishnamoorti, R. Macromolecules 2000, 33, 3739.
17. Ding, C.; Jia, D.; He, H.; Guo, G.; Hong, H. Polym Test 2005, 24, 94.
18. Rockwood additives, Southern Clay Products Inc. Available at: www.nanoclay.com/selection_chart.asp.
19. Garcia-Lopez, D.; Picazo, O.; Merino, J. C.; Pastor, J. M. Eur Polym Mater 2003, 39, 945.
20. Li, J.; Zhou, C. X.; Wang, G.; Zhao, D. L. J Appl Polym Sci 2003, 89, 3609.
21. Morgan, A. B.; Harris, J. D. Polymer 2003, 44, 2313.
22. Sheng, N.; Boyce, M. C.; Parks, D. M.; Rutledge, G. C.; Abes, J. I.; Cohen, R. E. Polymer 2003, 42, 9929.
23. Fornes, T. D.; Paul, D. R. Polymer 2003, 44, 4993.
24. Tucker, C. L.; Liang, E. Compos Sci Technol 1999, 59, 655.
25. Halpin, J. C.; Kardos, J. L. Polym Eng Sci 1976, 16, 344.
26. Weon, J. I.; Sue, H. J. Polymer 2005, 46, 6325.